British Journal of Pharmacology (2007) 151, 84–95
 0007–1188/07 $30.00
www.brjpharmacol.org

RESEARCH PAPER

Direct labelling of the human $P2X_7$ receptor and identification of positive and negative cooperativity of binding

AD Michel[1], LJ Chambers[1], WC Clay[2], JP Condreay[2], DS Walter[1] and IP Chessell[1]

[1]*Neurology & GI Centre of Excellence for Drug Discovery, GlaxoSmithKline Research and Development Limited, Harlow, Essex, UK and* [2]*Department of Biochemical & Cellular Targets, Molecular Discovery Research, GlaxoSmithKline, NC, USA*

Background and Purpose: The $P2X_7$ receptor exhibits complex pharmacological properties. In this study, binding of a [^{3}H]-labelled $P2X_7$ receptor antagonist to human $P2X_7$ receptors has been examined to further understand ligand interactions with this receptor.
Experimental Approach: The $P2X_7$ receptor antagonist, *N*-[2-({2-[(2-hydroxyethyl)amino]ethyl}amino)-5-quinolinyl]-2-tricyclo[3.3.1.1^{3,7}]dec-1-ylacetamide (compound-17), was radiolabelled with tritium and binding studies were performed using membranes prepared from U-2 OS or HEK293 cells expressing human recombinant $P2X_7$ receptors.
Key Results: Binding of [^{3}H]-compound-17 was higher in membranes prepared from cells expressing $P2X_7$ receptors than from control cells and was inhibited by ATP suggesting labelled sites represented human $P2X_7$ receptors. Binding was reversible, saturable and modulated by $P2X_7$ receptor ligands (Brilliant Blue G, KN62, ATP, decavanadate). Furthermore, ATP potency was reduced in the presence of divalent cations or NaCl. Radioligand binding exhibited both positive and negative cooperativity. Positive cooperativity was evident from bell shaped Scatchard plots, reduction in radioligand dissociation rate by unlabelled compound-17 and enhancement of radioligand binding by KN62 and unlabelled compound-17. ATP and decavanadate inhibited binding in a negative cooperative manner as they enhanced radioligand dissociation.
Conclusions: These data demonstrate that human $P2X_7$ receptors can be directly labelled and provide novel insights into receptor function. The positive cooperativity observed suggests that binding of compound-17 to one subunit in the $P2X_7$ receptor complex enhances subsequent binding to other $P2X_7$ subunits in the same complex. The negative cooperative effects of ATP suggest that ATP and compound-17 bind at separate, interacting, sites on the $P2X_7$ receptor.
British Journal of Pharmacology (2007) **151,** 84–95. doi:10.1038/sj.bjp.0707196; published online 5 March 2007

Keywords: $P2X_7$ receptor; radioligand binding; ATP; KN62; PPADS; Suramin; BzATP

Abbreviations: BzATP, 2′- and 3′-*O*-(4benzoylbenzoyl) ATP; BBG, brilliant blue G (Coomassie brilliant blue); BSA, bovine serum albumien; Compound-17, *N*-[2-({2-[(2-hydroxyethyl)amino]ethyl}amino)-5-quinolinyl]-2-tricyclo[3.3.1.1^{3,7}]dec-1-ylacetamide; OxATP, periodate oxidised ATP; NSB, nonspecific binding; PBS, phosphate-buffered saline; PPADS, pyridoxalphosphate-6-azophenyl-2′,4′-disulphonic acid

Introduction

The $P2X_7$ receptor has intriguing biophysical properties, activates a diverse range of cellular events and mediates a wide range of functional effects (North, 2002; Egan *et al*., 2006; Gever *et al*., 2006).

The pharmacological properties of this receptor are complex, both with respect to agonist and antagonist effects. In functional studies, the $P2X_7$ receptor is usually only activated by high concentrations of ATP (high μM to mM) and by slightly lower concentrations of 2′- and 3′-*O*-(4benzoylbenzoyl) ATP (BzATP). Agonist potency at the $P2X_7$ receptor is highly sensitive to the ionic composition of physiological solutions and can be increased by removing calcium and magnesium ions and even NaCl from these solutions (Cockcroft and Gomperts, 1979; Wiley *et al*., 1992; Surprenant *et al*., 1996; Michel *et al*., 1999). In addition, agonist concentration–effect curves derived from studies on the $P2X_7$ receptor are very steep (Surprenant *et al*., 1996; Michel *et al*., 1999). This phenomenon is also observed for several other P2X receptors and may reflect cooperative interactions between ATP-binding sites, presumably on adjacent subunits of the P2X receptor complex (Bean,

Correspondence: Dr AD Michel, Neurology & GI Centre of Excellence for Drug Discovery, GlaxoSmithKline Research & Development Limited, New Frontiers Science Park, Third Avenue, Harlow, Essex, CM19 5AW, UK.
E-mail: adm7393@gsk.com
Received 11 December 2006; revised 16 January 2007; accepted 19 January 2007; published online 5 March 2007

1992). This would be consistent with structural studies, which suggest that $P2X_1$, $P2X_2$ and $P2X_4$ receptor subtypes are each composed of three identical P2X subunits (Aschrafi *et al*., 2004; Barrera *et al*., 2005). It is not known if the same trimeric structure applies to the $P2X_7$ receptor, but would seem plausible, and so positive cooperative interactions between subunits may explain the steep ATP concentration–effect curves observed in studies on the $P2X_7$ receptor.

A number of antagonists of the $P2X_7$ receptor have been described (North, 2002; Gever *et al*., 2006) but their interaction with the receptor is seldom competitive, and there are discrepancies in potency between studies and many of the antagonists display considerable species differences in potency. For example, the prototypic P2X antagonist suramin, blocks $P2X_7$ receptors in some studies (Hibell *et al*., 2001) but not in others (Bianchi *et al*., 1999). Similarly, pyridoxalphosphate-6-azophenyl-2′,4′-disulphonic acid (PPADS) is a potent antagonist of $P2X_7$ receptors in some studies (Chessell *et al*., 1998; Michel *et al*., 2000) but not in others (Rassendren *et al*., 1997). This may reflect the atypically slow onset of action of PPADS at $P2X_7$ receptors (Chessell *et al*., 1998). The ATP analogue, periodate oxidised ATP (oxATP), is a $P2X_7$ receptor antagonist (Murgia *et al*., 1993) but it is irreversible, requires prolonged incubation and is neither selective for $P2X_7$ receptors over other P2X receptor types (Evans *et al*., 1995) nor is it a specific P2X antagonist (Beigi *et al*., 2003). Furthermore, it exhibits species differences in potency and its potency is affected by the ionic composition of physiological solutions (Hibell *et al*., 2001).

Although PPADS, oxATP and suramin are not selective antagonists of the $P2X_7$ receptor, a number of selective $P2X_7$ receptor antagonists have been described. KN62, a known calmodulin kinase II inhibitor, is a potent antagonist of human $P2X_7$ receptors (Gargett and Wiley, 1997) but exhibits lower potency at mouse $P2X_7$ receptors and has no effect at rat $P2X_7$ receptors (Humphreys *et al*., 1998; Hibell *et al*., 2001). Brilliant blue G ((BBG) also known as Coomassie brilliant blue) is a potent and selective antagonist of rat and mouse PX_7 receptors (Jiang *et al*., 2000; Hibell *et al*., 2001). However, neither of these compounds functions as a simple competitive antagonist. Both compounds have slow dissociation rates (Jiang *et al*., 2000; Michel *et al*., 2006a) and KN62 may be an allosteric inhibitor as it produces saturable, noncompetitive antagonist effects at human and mouse $P2X_7$ receptors (Humphreys *et al*., 1998; Michel *et al*., 2000).

We have found that decavanadate is a potent antagonist of $P2X_7$ receptors and that, in contrast to other $P2X_7$ receptor antagonists, it acts as a competitive antagonist in functional studies (Michel *et al*., 2006a). Although decavanadate is not a specific P2X antagonist, nor is it selective for $P2X_7$ receptors, it is a useful tool for studying $P2X_7$ receptors and has been used to provide indirect evidence that decavanadate, oxATP and PPADS, but not KN62, interact with the ATP binding site of the $P2X_7$ receptor (Michel *et al*., 2006a).

A number of structurally novel, high affinity, potent and selective, $P2X_7$ receptor antagonists have been described in patents in the last few years (Romagnoli *et al*., 2005). In this study, we have radiolabelled one of these compounds, *N*-[2-({2-[(2-hydroxyethyl)amino]ethyl}amino)-5-quinolinyl]-2-tricyclo[3.3.1.1^{3,7}]dec-1-ylacetamide (compound-17; Ford *et al*., 2003) to determine if it can directly label the $P2X_7$ receptor and be used to study the interactions of ligands with this receptor.

Methods

Preparation of the human $P2X_7$ receptor recombinant BacMam construct

The human $P2X_7$ receptor sequence (Rassendren *et al*, 1997) was excised from the plasmid pCDNA3 using the restriction enzymes *Hin*dIII and *Not*I, and then ligated into the *Hin*dIII/*Not*I sites of the pFastBac-Mam-1 vector (Condreay *et al*., 1999). Recombinant baculovirus stocks of BacMam-hu$P2X_7$ virus were prepared in Sf9 cells using standard propagation methods as described previously (Clay *et al*., 2003).

Cell culture and membrane preparation

HEK293 cells expressing human recombinant $P2X_7$ receptors (HEK293-$P2X_7$ cells) were cultured as described previously (Michel *et al*., 2000). Cells were grown to confluence, rinsed with phosphate-buffered saline (PBS), harvested by incubation in versene for 10 min and then centrifuged at 200 *g* for 5 min. The human $P2X_7$ receptor was also recombinantly expressed in the human U-2 OS osteosarcoma cell line (ATCC# HTB-96) by direct overlay of BacMam-hu$P2X_7$ virus as described previously (Ames *et al*., 2004). Briefly, U-2 OS cells were grown as a monolayer culture at 37°C in a humidified atmosphere (95% air and 5% CO_2) in Dulbecco's modified Eagle's medium (DMEM)/F12 medium supplemented with 10% fetal calf serum. Cells were grown to confluence in T175 flasks and then treated with BacMam-hu$P2X_7$ virus for 24 h (6.2×10^8 plaque-forming units per T175 flask). Thereafter, the cells were rinsed with PBS, incubated for 10 min in versene, harvested and centrifuged at 200 *g* for 5 min.

To prepare membranes, cell pellets from up to 10 T175 flasks of cells were resuspended in 35 ml of 50 mM Tris-HCl, 140 mM NaCl, 5 mM Na_2-ethylenediaminetetraacetic acid (EDTA) buffer (pH 7.4 at 4°C) and homogenised using a polytron P10 (2×10 s bursts at full speed). The homogenate was centrifuged at 20 000 r.p.m. in a Sorval Eureka centrifuge at 4°C for 20 min (SS34 rotor – approximately 48 000 *g*). The pellet was rinsed with water, resuspended in assay buffer (50 mM Tris-HCl, pH 7.4) and centrifuged as before. The final cell pellet was resuspended in assay buffer and frozen at −80°C until required.

Membranes were also prepared from wild-type HEK293 cells and from wild-type and mock transduced U-2 OS cells using the same procedure. For mock transductions a BacMam virus expressing the CRE-Luciferase reporter gene construct (CRE-Luc, Montminy *et al*., 1986; Bouaboula *et al*., 1997) was used.

Radioligand-binding assays

Membranes and radioligand (0.05–40 nM) were incubated in polypropylene tubes in a final volume of 200 μl of 50 mM Tris-HCl assay buffer, pH 7.4, at room temperature (19–22°C). Nonspecific binding (NSB) was routinely defined

using 10 μM unlabelled compound-17. In some studies (Figure 2), NSB was also defined using 100 μM ATP. Reactions were conducted at room temperature for the indicated times before separating bound and free radioligand by vacuum filtration, using a Brandell cell harvester, through 96-well GF/B glass fibre filters (Perkin-Elmer, Beaconsfield, Bucks, UK) pretreated with 0.3% polyethyleneimine (PEI) before use. Filters were washed with 3×2 ml aliquots of ice-cold water. The use of PEI was essential to reduce the high levels of filter binding that otherwise occurred. Filters were dried, 50 μl of microscint O (Perkin-Elmer) was added and radioactivity bound was determined using a Perkin-Elmer Topcount scintillation counter. The counts per minute (CPM) values from the Topcount were converted into disintegration per minute (DPM) values using an externally generated quench curve. In some studies in which radioligand solutions were used more than 15 min after preparation, 0.01% bovine serum albumin (BSA) was included in radioligand solutions to prevent adhesion of radioligand to plastic tubes. This was not required in most studies where radioligands and compounds were added directly to assay tubes as the protein in membrane preparations was sufficient to prevent adhesion of radioligand to plastic tubes (AD Michel, unpublished observation). Inclusion of 0.01% BSA in the assay buffer did not affect the radioligand K_D or competition curves for compound-17, a monoclonal antibody raised against the extracellular domain of the human $P2X_7$ receptor ($P2X_7$ mAb, Buell *et al*., 1998), KN62 or BBG (AD Michel, unpublished observation).

Experimental design

In saturation binding studies, the radioligand concentration was varied between 0.05 and 40 nM and radioligand binding determined after 60–240 min (routinely 120 min). In studies to investigate if radioligand depletion was occurring, reactions were performed in final assay volumes of 200–800 μl while maintaining the receptor amount constant. In association studies, radioligand (0.1–5 nM) and membranes, with or without 10 μM compound-17, were incubated for varying times before filtration. In competition studies, radioligand, membranes and competing compounds were incubated for 1 h at room temperature before terminating incubations by vacuum filtration. For these competition studies either a low (0.3 nM) or high (2 nM) radioligand concentration was employed.

To examine the ability of oxATP or PPADS to block the effects of ATP on radioligand binding (see Figure 7), membranes were incubated with buffer or antagonists for 60 min at either 37°C (oxATP) or room temperature (PPADS) before adding ATP and radioligand. After 60 min co-incubation, bound and free ligand were separated as described above.

In dissociation studies, radioligand (2 nM) and membranes were incubated for 60 min at room temperature. Thereafter, 0.1 ml aliquots of the reaction mixture was diluted with 2 ml of assay buffer and dissociation allowed to proceed for varying times at room temperature before separating bound and free radioligand by vacuum filtration. In some dissociation studies, 2 ml of assay buffer used to initiate dissociation also contained the indicated concentrations of compounds.

Data analysis

In all studies, NSB was defined as the difference between binding in the absence and presence of 10 μM compound-17. Specific binding was analysed using GraphPad Prism 3.0 by GraphicPad Software Inc. (San Diego, CA, USA) to estimate binding parameters. Binding was analysed according to models assuming binding to single or multiple populations of noninteracting sites. In Figure 8b, binding measured after 30 min dissociation in the absence of compounds was defined as 100% and that after 30 min in the presence of 100 μM BzATP as 0%. Other data were expressed relative to these values.

Results are shown as the mean $\pm$ s.e.m. of 3–6 experiments conducted in duplicate. Differences between means was assessed by one-way analysis of variance (ANOVA) with Dunnett's test; values of $P<0.05$ were taken as showing a significant difference.

Materials

Compound-17 was prepared from the precursor ethyl *N*-[2-({5-[(tricyclo[3.3.1.1^{3,7}]dec-1-ylacetyl)amino]-2-quinolinyl}amino)ethyl]glycinate (Figure 1). The precursor (0.05 g and 0.11 mmol) was dissolved in tetrahydrofuran (1.5 ml) and 1 M lithium aluminium hydride in tetrahydrofuran (0.32 ml, 0.32 mmol, 3 equiv.) was added dropwise and the reaction was stirred at room temperature for 2.5 h. The mixture was then extracted with 3:1 chloroform/isopropanol (12 + 5 ml). The combined organic extracts were concentrated and then purified by high-pressure liquid chromatography (HPLC) to yield compound-17 as a white solid. For synthesis of [^{3}H]compound-17, the above reactions were performed using tritium-labelled lithium aluminium hydride by Tritec (Switzerland). The specific activity of the radioligand was 2.1 TBq mmol^{-1} and the purity >99% (HPLC).

ATP, BBG, BzATP, KN62, PPADS, oxATP, sodium orthovanadate and suramin were obtained from Sigma (Poole,

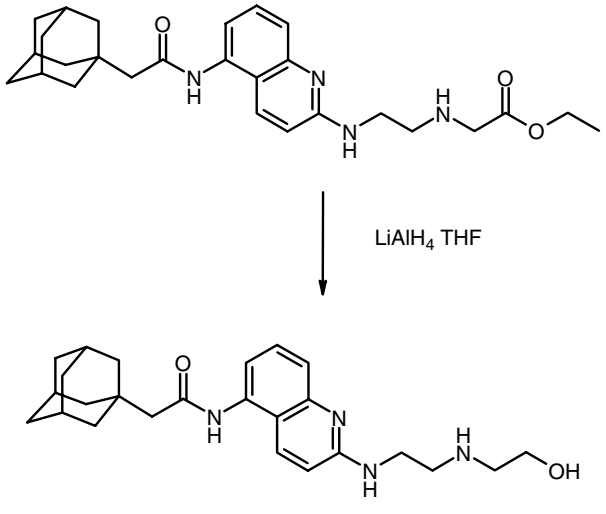

Compound-17

Figure 1 Synthesis and structure of compound-17.

Dorset, UK). The pH of ATP and oxATP solutions was adjusted to pH 7.4 with NaOH before use. The preparation of the P2X$_7$ mAb (Buell *et al*., 1998) and decavanadate (Michel *et al*., 2006a) have been described previously. All cell-culture reagents were from Invitrogen (Paisley, UK).

Results

Binding of [^{3}H]compound-17 to membranes from wild-type and P2X$_7$ receptor expressing cells

In membranes from wild-type HEK293 cells there were low levels of specific binding, as defined using 10 μM compound-17, but no specific binding as defined using 100 μM ATP (Figure 2). In contrast, in membranes from HEK293-P2X$_7$ cells, there were much higher levels of specific binding of [^{3}H]compound-17, as defined using 10 μM compound-17, and appreciable levels of specific binding, as defined using 100 μM ATP (Figure 2).

We also examined radioligand binding in a second cell line using the BacMam transient expression system. Membranes from mock-transfected U-2 OS cells (Figure 2) and wild-type U-2 OS cells (data not shown) had no ATP-displaceable specific binding and nonsignificant levels of 10 μM compound-17 displaceable specific binding. In contrast, membranes from U-2 OS cells transduced with human P2X$_7$ receptors using the BacMam expression system exhibited high levels of specific binding defined using either 100 μM ATP or 10 μM compound-17 (Figure 2).

These data suggest that [^{3}H]compound-17 can label human P2X$_7$ receptors, either stably expressed or after transient expression using the BacMam expression system. For further studies, NSB was defined using 10 μM compound-17. The specific binding defined in this manner may contain a small component ($\sim$0–7%) of non-P2X$_7$ receptor binding. The majority of studies used membranes prepared from HEK293-P2X$_7$ cells.

Kinetics of binding

Kinetic experiments (Figure 3) showed that binding of 0.15–5 nM. [^{3}H]compound-17 was relatively rapid in onset and achieved equilibrium within 30–128 min. At each radioligand concentration, binding at 128 min was not significantly different from that measured at 256 min. These data demonstrate that radioligand binding is relatively rapid in

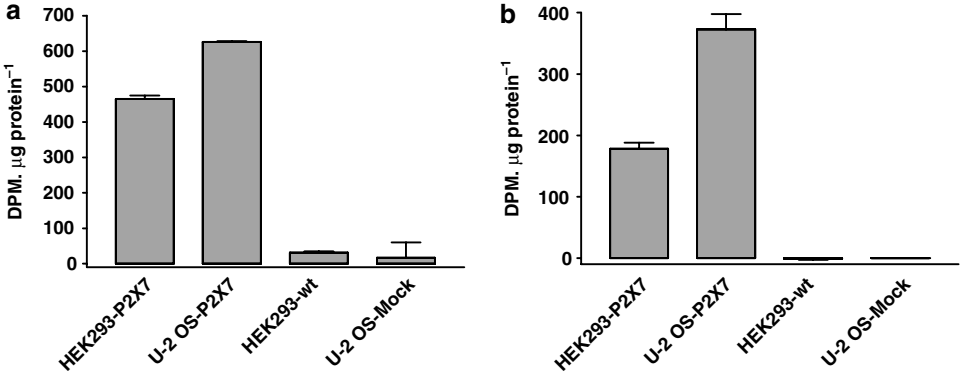

Figure 2 Specific binding of [^{3}H]compound-17 to membranes prepared from HEK293 cells stably expressing the human P2X$_7$ receptor (HEK293-P2X7), wild-type HEK293 cells (HEK293-wt), U-2 OS cells transduced with BacMam-huP2X7 virus (U-2 OS-P2X7) or U-2 OS cells transduced with BacMam-CRE-luciferase virus as control (U-2 OS-Mock). (**a**) Specific binding defined using 10 μM compound-17. (**b**) Specific binding defined using 100 μM ATP. The data are from a single experiment typical of two other experiments.

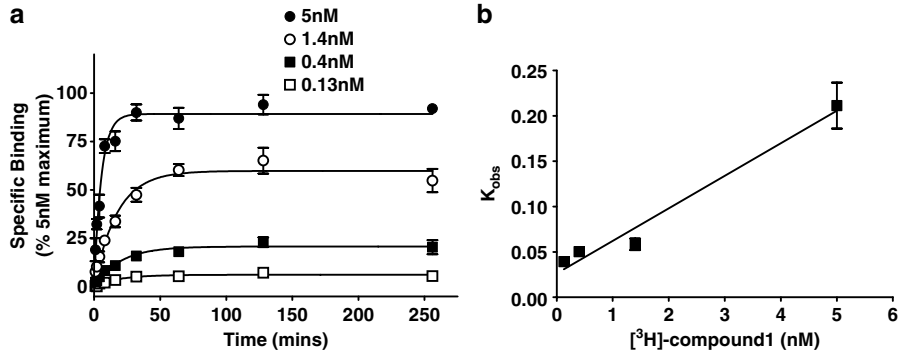

Figure 3 Association of [^{3}H]compound-17 with membranes prepared from HEK293 cells stably expressing the human P2X$_7$ receptor. Specific binding was defined with 10 μM compound-17. (**a**) Specific binding was measured at the indicated time points at the four concentrations of radioligand. (**b**) The K_{obs} values from (**a**) are plotted against radioligand concentration. The *Y*-axis intercept was 0.026. The data are the mean $\pm$ s.e.m. of 3–4 experiments.

onset and stable for at least 2–4 h. Observed rates of association (K_{obs}) increased with increasing radioligand concentrations (Figure 3b) and the $t_{1/2}$ values were 17.9 ± 2.2, 14.1 ± 1.2, 12.4 ± 1.5 and 3.4 ± 0.4 min, respectively, at radioligand concentrations of 0.14, 0.4, 1.4 and 5 nM. A plot of K_{obs} values vs radioligand concentration (Figure 3b) yielded a K_1 value of 0.026, which was similar to the value of 0.023 determined in dissociation studies (see below). The kinetically derived K_D values from these association experiments, calculated using the K_1 value of 0.023 from dissociation studies and the K_{+1} values calculated from the association experiments, were 0.6, 1.0 and 0.3 nM at radioligand concentrations of 5, 1.4 and 0.5 nM, respectively.

Saturation binding of [^{3}H]compound-17

In membranes from HEK293-P2X$_7$ cells, radioligand binding increased with increasing radioligand concentrations up to ~40 nM and at this radioligand concentration, binding was approaching saturation (Figure 4). Specific binding at radioligand concentrations below 1 nM was complex (see below) and so the initial analysis of binding only examined binding at radioligand concentrations >1 nM. In three of six experiments, these specific-binding data could be analysed by assuming binding to a single population of sites, whereas in the other three experiments, there was evidence of upward concave curvature in the Scatchard plot (Figure 4b, furthest right data points). For those experiments, specific-binding data could be better described by assuming that the radioligand was labelling a single population of high-affinity sites and an additional nonsaturable component of binding. The high-affinity sites were characterised by a K_D of 1.4 ± 0.15 nM and receptor density (B_{max}) of 5.43 ± 0.55 pmol mg^{-1} protein. In view of the complexity of binding (see below), and the high levels of NSB, the low-affinity sites labelled at high radioligand concentrations were not examined further. Similar results were obtained when using membranes from U-2 OS cells transduced with the human P2X$_7$ receptor using the BacMam viral expression system ($K_D = 1.1 \pm 0.25$ nM, $B_{max} = 5.73 \pm 0.55$ pmol mg^{-1} protein).

Pharmacological characterisation of [^{3}H]compound-17 binding sites

Binding of [^{3}H]compound-17 was affected by a variety of P2 agonists and antagonists including ATP, BzATP, BBG, KN62, decavanadate, suramin and the P2X$_7$ mAb (Figures 5 and 6). Note that high concentrations of PPADS, BBG and decavanadate could not be studied owing to colour quenching which could not reliably be corrected on the Topcount scintillation counter. Thus, when using concentrations of compounds that quenched scintillation counting by more than 70%, the corrected DPM values suggested that these

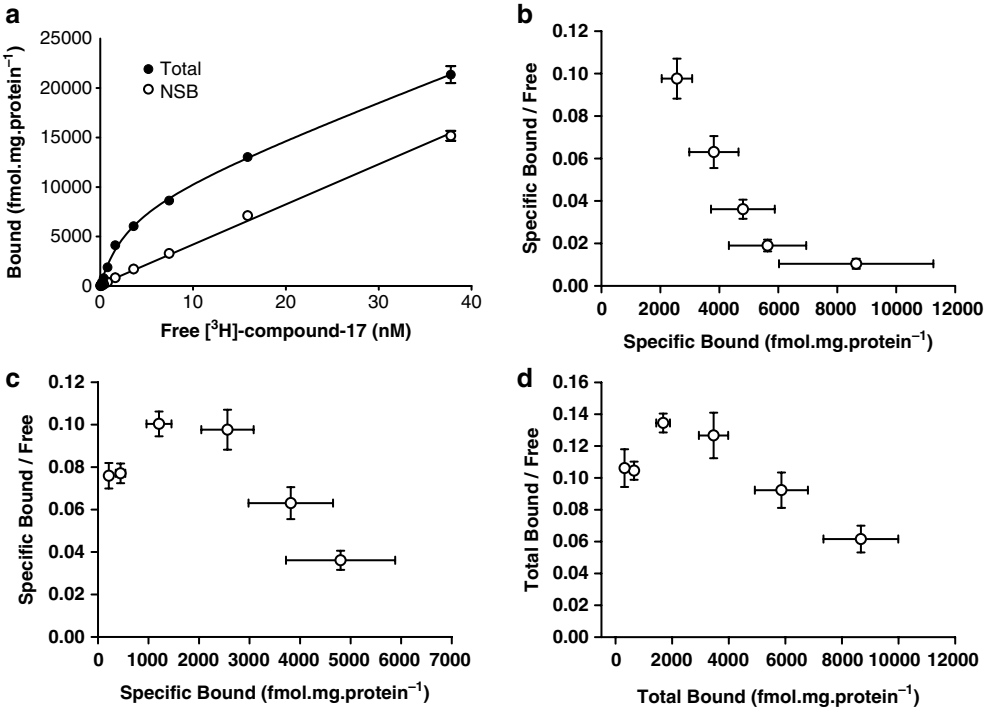

Figure 4 Saturation analysis for [^{3}H]compound-17 binding to membranes prepared from HEK293 cells stably expressing the human P2X$_7$ receptor. Specific binding was defined with 10 μM compound-17. (**a**) Total and NSB from a representative experiment was measured at the indicated radioligand concentrations (0.15–38 nM). Data are mean ± s.e.m. of the triplicate samples for this experiment. (**b**) Composite Scatchard plot of the specific binding data using radioligand concentrations from approximately 1 to 38 nM ($n = 6$). (**c**) Composite Scatchard plot of the specific binding data using radioligand concentrations from ~0.15 to 7 nM ($n = 6$). (**d**) Composite Scatchard plot of the total binding data using radioligand concentrations from ~0.15 to 7 nM ($n = 6$).

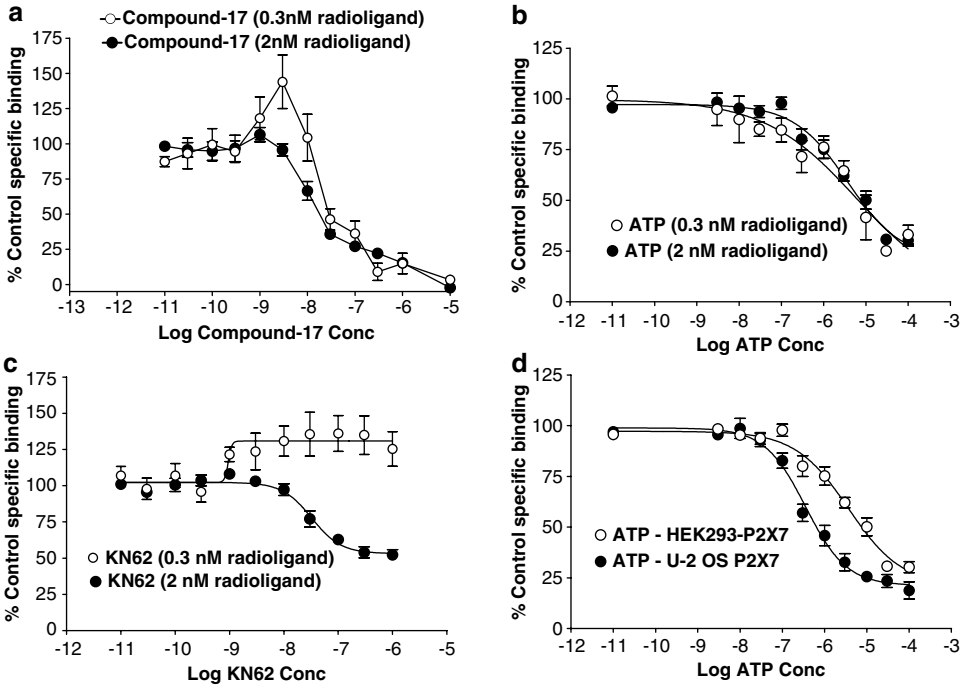

Figure 5 Competition studies performed at 0.3 or 2 nM [^{3}H]compound-17. Studies were performed using membranes prepared from HEK293 cells stably expressing the human P2X$_7$ receptor (**a–d**) or from U-2 OS cells transduced with the human P2X$_7$ receptor using the BacMam expression system (**d**). Specific binding was defined with 10 μM compound-17. (**a**) Effect of compound-17 at 0.3 and 2 nM radioligand. (**b**) Effect of ATP at 0.3 and 2 nM radioligand. (**c**) Effect of KN62 at 0.3 and 2 nM radioligand. (**d**) Effect of ATP against 2 nM radioligand in membranes from U-2 OS or HEK293 cells. The data are the mean $\pm$ s.e.m. of 3–5 experiments.

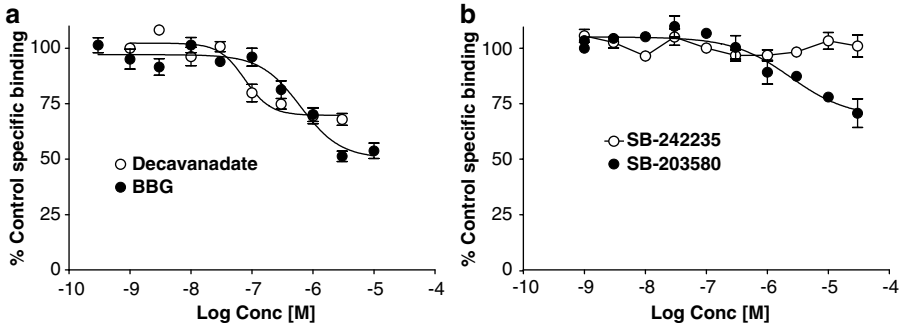

Figure 6 Competition by P2 receptor ligands for [^{3}H]compound-17 binding to membranes prepared from HEK293 cells stably expressing the human P2X$_7$ receptor. Sites were labelled using 2 nM [^{3}H]compound-17. Specific binding was defined with 10 μM compound-17. (**a**) Effect of BBG or decavanadate. (**b**) Effect of SB-203580 or SB-242235. The data are the mean $\pm$ s.e.m. of 3–4 experiments.

compounds were potentiating binding by more than 200% in some cases (data not shown).

The initial radioligand characterisation was performed using ATP, KN62 and compound-17. When using low concentrations of radioligand (0.3 nM), KN62 ($pEC_{50} = 9.01 \pm 0.29$) enhanced binding by $40 \pm 13\%$ (Figure 5c), whereas ATP ($pIC_{50} = 5.95 \pm 0.37$) inhibited binding by $68 \pm 2\%$ (Figure 5b). Compound-17 enhanced binding at a concentration of 3 nM ($P < 0.05$, one-way ANOVA with Dunnett's test) but at higher concentrations inhibited binding with pIC_{50} of 7.48 ± 0.10 (Figure 5a).

When using a higher radioligand concentration of 2 nM, most compounds inhibited binding. KN62 ($pIC_{50} = 7.55 \pm 0.09$) and ATP ($pIC_{50} = 5.73 \pm 0.07$) inhibited binding by 46 ± 5 and $68 \pm 2\%$, respectively (Figure 5c and b). Compound-17 inhibited $83 \pm 3\%$ of specific binding with high affinity ($pIC_{50} = 7.86 \pm 0.13$) and inhibited the remaining binding sites with a pIC_{50} of 5.65 ± 0.12 (Figure 5a). Identical results were generally obtained when using membranes from U-2 OS cells transduced with the human P2X$_7$ receptor using the BacMam expression system (data not shown). The only exception was with ATP, which possessed slightly higher potency than in membranes from HEK293-P2X$_7$ cells (Figure 5d).

Binding of 2 nM radioligand was also partially inhibited by BzATP ($pIC_{50} = 6.84 \pm 0.09$; $73 \pm 2\%$ inhibition, data not shown), BBG ($pIC_{50} = 6.23 \pm 0.10$; $50 \pm 3\%$ inhibition) and decavanadate ($pIC_{50} = 7.03 \pm 0.15$; $32 \pm 3\%$ inhibition)

(Figure 6a). SB-203580, but not SB-242235 blocks P2X$_7$ receptor-mediated ethidium accumulation in cells expressing human P2X$_7$ receptors (Michel *et al*., 2006b). SB-203580, but not SB-242235, partially inhibited radioligand binding ($pIC_{50} = 5.59 \pm 0.12$, $34 \pm 9\%$ inhibition; Figure 6b). The P2X$_7$ mAb inhibited $45 \pm 3\%$ of binding with high affinity ($pIC_{50} = 7.15 \pm 0.14\,g\,ml^{-1}$; $IC_{50} = 0.07\,\mu g\,ml^{-1}$). Suramin enhanced total and specific binding at concentrations from 1 to 10 μM, but at higher concentrations (30 and 100 μM), it slowed down the rate of filtration while harvesting membranes to separate bound and free radioligand. Consequently its effects could not be easily studied.

Neither PPADS (0.01–10 μM) nor oxATP (0.01–1 mM) inhibited binding (data not shown). However, when these compounds were preincubated with membranes, they blocked the ability of ATP to inhibit binding (Figure 7). In both cases, the compounds produced an unsurmountable blockade of the ATP-induced inhibition of binding (Figures 7a and c). In Figures 7b and d, the ability of PPADS and oxATP to reverse the inhibition produced by ATP are shown. The PPADS pEC_{50} for blocking ATP inhibition of binding was 6.16 ± 0.37, 6.15 ± 0.2, 5.85 ± 0.12 and 5.57 ± 0.16 at ATP concentrations of 1, 3, 30 and 300 μM, respectively (Figure 7b). The oxATP pEC_{50} for blocking the ATP inhibition of binding was 4.78 ± 0.15, 4.79 ± 0.10, 4.48 ± 0.08 and 3.75 ± 0.16 at ATP concentrations of 1, 3, 30 and 300 μM, respectively (Figure 7d).

Pretreatment of membranes with 1 mM oxATP also blocked the ability of suramin to enhance radioligand binding but did not affect the inhibition of radioligand binding produced by KN62, BBG or the P2X$_7$ mAb (data not shown).

Evidence for positive cooperative interactions in saturation binding studies

Although the saturation data appear consistent with the radioligand predominantly binding to a single population of sites, when binding data obtained using radioligand concentrations lower than 1 nM were included in the Scatchard plot, a bell-shaped plot was observed in both specific (Figure 4c) and total (Figure 4d) binding data. This could result from radioligand depletion at low radioligand concentrations, membrane degradation at low radioligand concentrations, inadequate association time or positive cooperativity. Increasing assay volume fourfold to 800 μl, while maintaining the same amount of receptor added, or increasing incubation time to 4 h did not affect the shape of the Scatchard plot indicating that ligand depletion was not occurring and that equilibration time was adequate (data not shown). Furthermore, association experiments at low

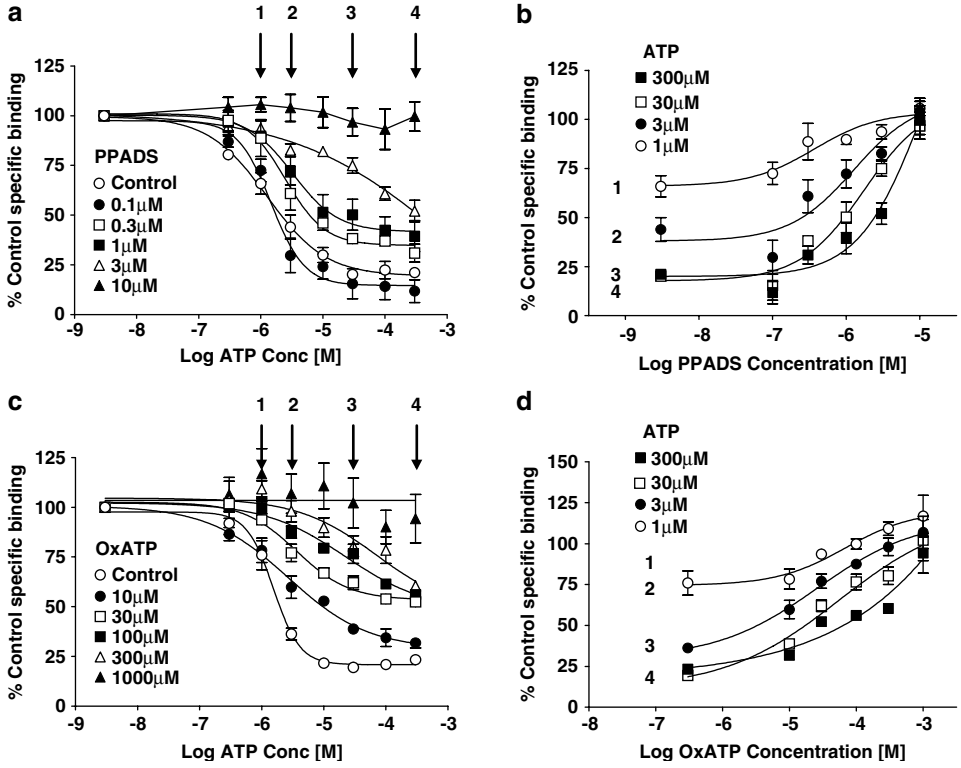

Figure 7 Effect of oxATP or PPADS on ATP inhibition of 2 nM [^{3}H]compound-17 binding. Studies were performed using membranes prepared from HEK293 cells stably expressing the human P2X$_7$ receptor. Specific binding was defined with 10 μM compound-17. Membranes were preincubated with PPADS (60 min at room temperature) or oxATP (60 min at 37°C) before addition of ATP and 2 nM [^{3}H]compound-17. After a 60 min coincubation at room temperature, specific binding was measured. (**a**) Effect of preincubation with PPADS on ATP inhibition of radioligand binding. Arrows represent ATP concentrations used to construct the plots in (**b**). (**b**) Reversal of ATP-inhibition of binding by PPADS at the concentrations of ATP indicated in (**a**) (1, 3, 30 and 300 μM ATP). (**c**) Effect of preincubation with oxATP on ATP inhibition of radioligand binding. Arrows represent ATP concentrations used to construct plots in (**d**). (**d**) Reversal of ATP inhibition of binding by PPADS at the concentrations of ATP indicated in (**a**) (1, 3, 30 and 300 μM ATP). The data are the mean ± s.e.m. of four experiments.

radioligand concentrations showed that binding attained equilibrium within 2 h (see above).

In some systems, receptors may be unstable and their stability is increased by high concentrations of radioligand and this may appear as positive cooperativity (Chamness and McGuire, 1975). This is unlikely in these assays. Thus, when high concentrations of radioligand (30 nM) were added to membranes exposed to low radioligand concentrations (0.3 nM) for 1 h, the level of binding achieved after a further 1 h incubation (8491 ± 653 DPM; $n = 3$) was identical to that observed when the converse protocol was utilised (8339 ± 1087 DPM; $n = 3$). The most likely explanation for the bell-shaped Scatchard plots is positive cooperativity.

Further evidence for positive cooperative interactions in kinetic studies

Dissociation of the radioligand, induced by a 20-fold dilution, was relatively slow with a K_{-1} of 0.023 ± 0.0015 and a $t_{1/2}$ of 31 ± 2.3 min (Figure 8).

De Lean and Rodbard (1979) have suggested that positive cooperativity can lead to increases in radioligand binding in competition studies when using low but not intermediate or high radioligand concentrations and that, in dissociation experiments, the presence of unlabelled compound should slowdown radioligand dissociation induced by infinite dilution. Both of these effects were observed. Thus, compound-17 produced a distinct increase in binding at 3 nM when using low but not higher radioligand concentrations (Figure 5a) and the presence of compound-17 slowed down radioligand dissociation (Figure 8). The pIC$_{50}$ for this latter effect was 8.16 ± 0.10.

Evidence for negative cooperative effects of ATP, BzATP and decavanadate

Because ATP and several other ligands only produced partial inhibition of radioligand binding (Figures 5 and 6), we examined the effects of ATP and these compounds on radioligand dissociation. As it can be seen from Figure 8b, ATP, decavanadate and BzATP produced a marked increase in radioligand dissociation rate. In the presence of ATP, the radioligand dissociation was biphasic (Figure 8a) and a major proportion of binding was lost by the shortest dissociation time measured in these assays (30 s).

When studied after 30 min of dissociation, the pIC$_{50}$ for ATP, BzATP and decavanadate to increase radioligand dissociation was 5.33 ± 0.06, 6.18 ± 0.05 and 7.40 ± 0.10, respectively (Figure 8b). These pIC$_{50}$ values are close to the pIC$_{50}$ values from the competition studies (within 0.3–0.7 log unit). ATP and BzATP increased radioligand dissociation to the same extent but decavanadate only partially increased radioligand dissociation (Figure 8b). BBG (0.1–3 μM), KN62 (1–1000 nM) and the P2X$_7$ mAb (0.001–1 μg ml^{-1}) did not affect radioligand dissociation kinetics (data not shown).

Ionic effects on binding

We have shown previously that divalent and monovalent cations affect agonist potency (Michel *et al*., 1999). These binding assays were performed in the absence of ions with the exception of 50 mM Tris and its associated HCl. When $CaCl_2$, $MgCl_2$ and NaCl were included in the assays, they produced a concentration-related decrease in both total and NSB but did not affect the potency of unlabelled compound-17 (data not shown). $CaCl_2$ and $MgCl_2$ decreased ATP potency (Figure 9a and b) but this effect was not competitive as the maximal inhibition produced by ATP was reduced, particularly by $CaCl_2$, and the Schild plot of the data (Figure 9d) possessed slopes less unity for both compounds ($MgCl_2$, $pA_2 = 5.29 \pm 0.61$ and Schild slope $= 0.64 \pm 0.08$; $CaCl_2$, $pA_2 = 4.86 \pm 0.38$ Schild slope $= 0.74 \pm 0.10$). NaCl also reduced ATP potency (Figure 9d) but its effects were complicated as ATP inhibition curves became biphasic in the presence of 62.5 and 125mM NaCl (Figure 9c).

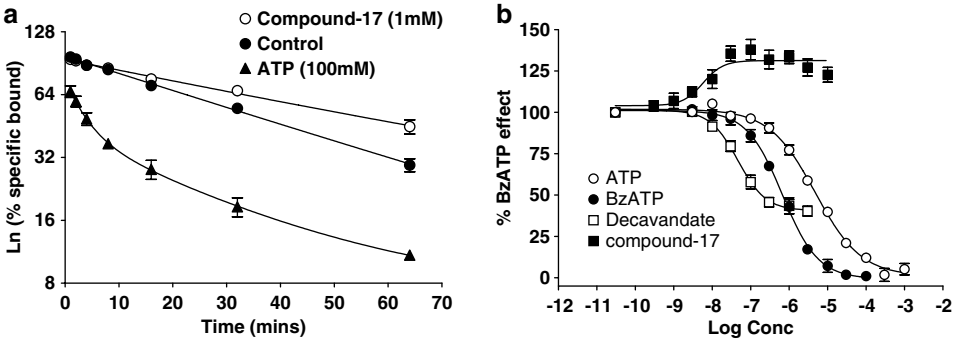

Figure 8 Effect of P2 receptor ligands on dissociation of [^{3}H]compound-17 binding to membranes prepared from HEK293 cells stably expressing the human P2X$_7$ receptor. Sites were labelled using 2 nM [^{3}H]compound-17 during a 1 h preincubation period. Dissociation was then initiated by addition of 2 ml of assay buffer to a 0.1 ml aliquot of the membrane-radioligand mixture and binding determined at various times thereafter either in the presence or absence of the indicated compounds. Specific binding was defined with 10 μM compound-17. (**a**) Dissociation of radioligand induced by dilution in the absence or presence of either ATP (100 μM) or compound-17 (1 μM). The data are expressed as a percentage of specific binding measured without radioligand dissociation. Note the semilogarithmic *Y*-axis scale. (**b**) Dissociation was measured after 30 min in the absence or presence of the indicated compounds. The binding measured in the absence of compounds (~50% dissociation) was assigned a value of 100% and the maximal increase in dissociation (~72% dissociation) produced by BzATP was assigned a value of 0%. The data for the compounds are expressed as a percentage of this BzATP effect. Data are the mean ± s.e.m. of 3–4 experiments.

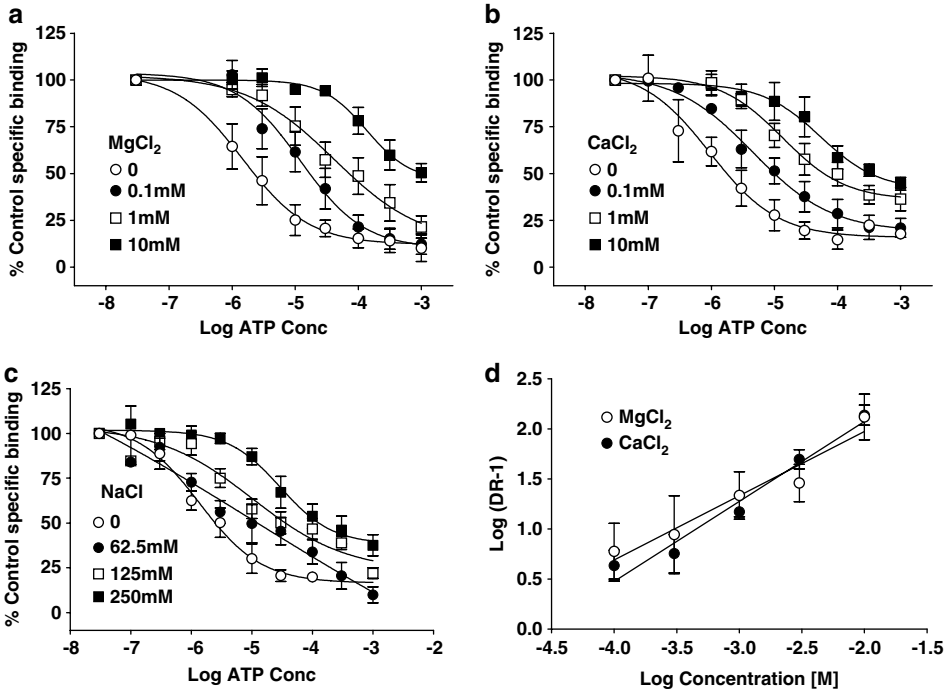

Figure 9 Effect of $MgCl_2$, $CaCl_2$ or NaCl on ATP inhibition of 2 nM [^{3}H]compound-17 binding. Studies were performed using membranes prepared from HEK293 cells stably expressing the human P2X$_7$ receptor. Specific binding was defined with 10 μM compound-17. ATP inhibition curves were determined in the absence or presence of the indicated concentrations of (**a**) $MgCl_2$, (**b**) $CaCl_2$ or (**c**) NaCl. (**d**) Schild plot for the effects of $MgCl_2$ and $CaCl_2$. For this figure, DR is the ratio of the ATP IC_{50} value in the presence of each concentration of $CaCl_2$ or $MgCl_2$ divided by the control ATP IC_{50} determined in the absence of these ions. The data are the mean$\pm$s.e.m. of 3–4 experiments.

Discussion

In this study, we have demonstrated that the human P2X$_7$ receptor can be labelled with [^{3}H]compound-17 and that the binding properties are complex and consistent with the compound binding in a positive cooperative manner to sites on the P2X$_7$ receptor which are distinct from, but coupled to, the ATP binding site.

The radioligand we have used is of moderate affinity (K_D $\sim$1 nM) but was able to label high-affinity sites in membranes from HEK293 or U-2 OS cells expressing a high density of human P2X$_7$ receptors ($\sim$5.5 pmol mg^{-1} protein). The radioligand may also label additional low-affinity sites in membranes from wild-type HEK293 and U-2 OS cells. However, these should only contribute to about 0–7% of the sites labelled after stable expression or transduction of the P2X$_7$ receptor and so were not examined further. Instead we characterised the high-affinity sites, as these exhibited properties consistent with their representing the human P2X$_7$ receptor (see below).

The properties of the high-affinity [^{3}H]compound-17 binding sites were complex as both positive and negative cooperativity of binding was detected. Positive cooperativity of binding was evident in saturation, kinetic and competition studies. Thus, we observed bell-shaped Scatchard plots in saturation studies, potentiation of binding by low concentrations of competing compounds when using low radioligand concentrations and a slowing of dissociation rate in the presence of unlabelled compound-17. All three of these observations are consistent with positive cooperativity and indeed are recognised diagnostic tests for cooperativity (De Lean and Rodbard, 1979). Although it is possible for various artefacts including ligand depletion, inadequate equilibration time or receptor degradation to appear as positive cooperativity, we ruled these out experimentally.

De Lean and Rodbard (1979) have developed mechanism free models to describe cooperative interactions in terms of effects on radioligand kinetics. In their models, the bell-shaped curvature in Scatchard plots and the enhancement of binding at low radioligand concentrations by competing compound are consistent with positive cooperativity arising from binding-induced effects on radioligand association. In addition, we found effects of unlabelled compound-17 on radioligand dissociation, suggesting that the positive cooperative interactions also lead to a slowing of radioligand dissociation. Hence, it would appear that the positive cooperative effects observed comprise both effects on radioligand association and dissociation.

We did not attempt to analyse our data in terms of a more mechanistic model. However, as discussed above the molecular structure of the P2X$_1$, P2X$_2$ and P2X$_4$ receptors have been suggested to be a trimeric association of subunits (Aschrafi *et al.*, 2004; Barrera *et al.*, 2005). If the structure of the P2X$_7$ receptor is also trimeric, then the simplest explanation for the cooperativity we observed is that binding of one molecule of radioligand to its site on a subunit in the P2X$_7$ receptor complex produces an increase in the affinity of the equivalent binding site on a second subunit. It should be noted that other models of cooperativity also predict bell-shaped Scatchard plots and potentiation of binding in

competition studies. The dimer-based model for G-protein-coupled receptors (Franco *et al*., 2005) also predicts this property but it appears to be a formally equivalent model to that postulated above, as it describes multiple-linked subunits. Of more relevance may be the multisubsite model for multivalent ligands (De Lean *et al*, 1979). This model, which does not invoke cooperativity, predicts bell-shaped Scatchard plots and also predicts effects of compounds on radioligand dissociation (Prinz and Striessnig, 1993). However, this model predicts that compounds should enhance, rather than inhibit, radioligand dissociation, and this contrasts with the ability of compound-17 to slow radioligand dissociation.

The pharmacology of the high-affinity binding sites was broadly consistent with that expected of the $P2X_7$ receptor. Binding was inhibited by known $P2X_7$ receptor ligands such as KN62, CBB, ATP, BzATP, decavanadate and the $P2X_7$ mAb. For the agonists, ATP and BzATP, potency estimates were higher than observed in functional studies but this probably reflects ionic composition of assay buffers (see below). For the antagonists, effective concentrations to inhibit binding were similar to those active in functional studies conducted in low ionic strength buffers and in the presence of low concentrations of divalent cations (Table 1). PPADS and oxATP did not directly inhibit binding (see below) but did block ATP inhibition of binding at concentrations similar to (oxATP) or slightly lower than (PPADS) those active in functional studies (Table 1).

ATP, BzATP, decavanadate, oxATP and PPADS appeared to bind to a site on the $P2X_7$ receptor, presumably the ATP binding site, that is distinct from the site at which compound-17 binds. Thus, ATP, BzATP and decavanadate only inhibited 30–75% of radioligand binding. More importantly, all three compounds increased radioligand dissociation and this is one of the diagnostic tests for negative cooperative effects exerted through a separate site (De Lean and Rodbard, 1979). It should be noted that the multisubsite model for multivalent ligands (De Lean *et al*, 1979; Prinz and Striessnig, 1993) also predicts that compounds may increase the radioligand dissociation rate but this is manifest as a simple increase in dissociation rate, whereas in the presence of ATP, radioligand dissociation became tri-phasic. It is intriguing that decavanadate affected radioligand dissociation, even though it is a competitive antagonist of ATP and BzATP (Michel *et al*., 2006a). In contrast, other slowly reversible or irreversible antagonists such as oxATP and PPADS, which appear to bind at the same site as decavanadate (Michel *et al*., 2006a), did not directly affect radioligand binding. However, these agents did appear to interact at the same site as ATP as they blocked the ability of ATP to inhibit radioligand binding and their effects required prolonged preincubation as observed in functional studies (Chessell *et al*., 1998; Michel *et al*., 2000). It may be possible that decavanadate is a partial agonist at the ATP binding site in these studies, whereas oxATP and PPADS are silent antagonists.

KN62 produced marked increases in binding at low radioligand concentrations and only produced partial inhibition of binding at higher radioligand concentrations. We also found that BBG and the $P2X_7$ mAb partially inhibited binding. These compounds did not affect radioligand dissociation so they either only compete for a fraction of the high-affinity sites labelled by compound-17 or they may influence binding through a site that is distinct from the sites at which ATP or compound-17 bind.

The model of the $P2X_7$ receptor emerging from these binding studies is complex. However, the mechanism of action of KN62, BBG, ATP, BzATP and decavanadate suggested by these binding data is generally consistent with previous functional studies on the $P2X_7$ receptor. Thus, KN62 produces a noncompetitive and saturable antagonist effect in some studies on the $P2X_7$ receptor (Humphreys *et al*., 1998; Michel *et al*., 2000), which would be consistent with it functioning as a negative cooperative or allosteric inhibitor. Similar effects are observed with the $P2X_7$ mAb (Michel *et al*., 1999). Furthermore, we have shown that ATP, BzATP, oxATP, decavanadate and PPADS bind at the same site in functional studies and that this site is distinct from that at which KN62 and BBG bind (Michel *et al*., 2006a).

Finally, the potency of ATP and BzATP in these binding studies is considerably higher than observed in functional studies. This is similar to studies on $P2X_1$–$P2X_4$ receptor where we have suggested that this reflects labelling of high-affinity desensitised states of those receptors (Michel *et al*., 1997). It is unlikely that the same situation prevails at the $P2X_7$ receptor, as these receptors do not desensitise (North,

Table 1 Comparison of potency estimates in radioligand binding and functional studies

Compound	*Binding potency*	*Functional pIC_{50}*	*Reference*
KN62	7.6	7.5	Hibell *et al*. (2001)
OxATP	3.8–4.8[a]	5.4	Hibell *et al*. (2001)
BBG	6.2	6.9	Hibell *et al*. (2001)
P2X7 mAB[b]	0.07 $\mu g\,ml^{-1}$	0.1–0.2 $\mu g\,ml^{-1}$	Buell *et al*. (1998)
		0.03 $\mu g\,ml^{-1}$	Michel *et al*. (2000)
Decavanadate	7.0	7.4	Michel *et al*. (2006a)
PPADS	5.6–6.2[a]	7.3	Hibell *et al*. (2001)
SB-203580	5.6	6.2–4.8	Michel *et al*. (2006b)
SB-224435	<5	<5	Michel *et al*. (2006b)

The binding data are pIC_{50} values except for oxATP, PPADS and the $P2X_7$ mAb.
[a]For oxATP and PPADS, pEC_{50} values to reverse the inhibitory effect of various concentrations of ATP are shown. The functional data are pIC_{50} values from BzATP-stimulated ethidium bromide cellular accumulation studies conducted in the absence of NaCl and presence of sucrose buffer.
[b]For the $P2X_7$ mAb, the binding data are the IC_{50} values and the functional data an effective concentration range to block BzATP-induced interleukin-1β release from THP1 cells (Buell *et al*., 1998) or the IC_{50} to inhibit BzATP-induced ethidium bromide accumulation in HEK293-$P2X_7$ cells (Michel *et al*., 2000).

2002). Instead, the high affinity may reflect the absence of divalent cations and low concentration of monovalent ions in the assay buffer as ions are known to affect agonist potency at $P2X_7$ receptors (see Introduction), and we found that addition of $CaCl_2$, $MgCl_2$ or NaCl could reduce ATP potency. The effects of ions were not examined in detail but all three metal chlorides produced noncompetitive or complex effects. This may confirm previous suggestions that the effects of ions are through allosteric actions on the $P2X_7$ receptor (Virginio *et al*., 1997) rather than through simple chelation of ATP, as the latter effect should appear competitive.

Taken together the data suggest that ligands such as compound-17 bind to a site on the $P2X_7$ receptor that is distinct from that at which ATP binds. As a result of binding to this site, compound-17 affects similar sites on adjacent subunits in the $P2X_7$ receptor complex and increases their affinity for the ligand. The effects of ATP in binding studies are mediated at a site distinct from that recognised by compound-17, and it is probable that BzATP, decavanadate, oxATP and PPADS also interact at this site. As compound-17 is an antagonist in functional studies, it may be inferred that its binding produces changes in the receptor, presumably conformational, that either result in inhibition of ATP binding or block functional effects subsequent to ATP binding. BBG, KN62 and the $P2X_7$ mAb modulate compound-17 binding in a complex manner that has not yet been defined but it is conceivable they may produce their effects by binding to an additional site, or sites, on the $P2X_7$ receptor that are distinct from both the compound-17 and ATP-binding sites.

Conflict of interest

The authors are employed by GlaxoSmithKline.

References

Ames R, Nuthulaganti P, Fornwald J, Shabon U, van-der-Keyl H, Elshourbagy N (2004). Heterologous expression of G protein-coupled receptors in U-2 OS osteosarcoma cells. *Receptors Channels* **10**: 117–124.

Aschrafi A, Sadtler S, Niculescu C, Rettinger J, Schmalzing G (2004). Trimeric architecture of homomeric $P2X_2$ and heteromeric P2X1 + 2 receptor subtypes. *J Mol Biol* **342**: 333–343.

Barrera NP, Ormond SJ, Henderson RM, Murrell-Lagnado RD, Edwardson MJ (2005). Atomic force microscopy imaging demonstrates that $P2X_2$ receptors are trimers but that $P2X_6$ receptors do not oligomerize. *J Biol Chem* **280**: 10759–10765.

Bean BP (1992). Pharmacology and electrophysiology of ATP-activated ion channels. *Trends Pharmacol Sci* **13**: 87–90.

Beigi RD, Kertesy SB, Aquilina G, Dubyak GR (2003). Oxidized ATP (oATP) attenuates proinflammatory signaling via P2 receptor-independent mechanisms. *Br J Pharmacol* **140**: 507–519.

Bianchi BR, Lynch KJ, Touma E, Niforatos W, Burgard EC, Alexander KM *et al*. (1999). Pharmacological characterization of recombinant human and rat P2X receptor subtypes. *Eur J Pharmacol* **376**: 127–138.

Bouaboula M, Perrachon S, Milligan L, Canat X, Rinaldi-Carmona M, Portier M *et al*. (1997). A selective inverse agonist for central cannabinoid receptor inhibits mitogen-activated protein kinase activation stimulated by insulin or insulin-like growth factor 1. Evidence for a new model of receptor/ligand interactions. *J Biol Chem* **272**: 22330–22339.

Buell G, Chessell IP, Michel AD, Collo G, Salazzo M, Herren S *et al*. (1998). Blockade of human $P2X_7$ receptor function with a monoclonal antibody. *Blood* **92**: 3521–3528.

Chamness GC, McGuire WL (1975). Scatchard plots: common errors in correction and interpretation. *Steroids* **26**: 538–542.

Chessell IP, Michel AD, Humphrey PPA (1998). Effects of antagonists at the human recombinant $P2X_7$ receptor. *Br J Pharmacol* **124**: 1314–1320.

Clay WC, Condreay JP, Moore LB, Weaver SL, Watson MA, Kost TA *et al*. (2003). Recombinant baculoviruses used to study estrogen receptor function in human osteosarcoma cells. *Assay Drug Dev Technol* **1**: 801–810.

Cockcroft S, Gomperts BD (1979). ATP induces nucleotide permeability in rat mast cells. *Nature* **279**: 541–542.

Condreay JP, Witherspoon SM, Clay WC, Kost TA (1999). Transient and stable gene expression in mammalian cells transduced with a recombinant baculovirus vector. *Proc Natl Acad Sci USA* **96**: 127–132.

De Lean A, Munson PJ, Rodbard D (1979). Multi-subsite receptors for multivalent ligands. Application to drugs, hormones, and neurotransmitters. *Mol Pharmacol* **15**: 60–70.

De Lean A, Rodbard D (1979). Kinetics of cooperative binding. *Receptors: Comprehensive Treatise* O'Brien RD (ed). New York: Plenum, Vol 1, Chapter 4, pp 143–192.

Egan TM, Samways DSK, Li Z (2006). Biophysics of P2X receptors. *Pflügers Arch* **452**: 501–512.

Evans RJ, Lewis C, Buell G, Valera S, North RA, Surprenant A (1995). Pharmacological characterization of heterologously expressed ATP-gated cation channels (P2X purinoceptors). *Mol Pharmacol* **48**: 178–183.

Ford R, Leroux F, Stocks M (2003). Preparation of (adamantyl)(quinolinyl)amides as P2X7 receptor antagonists. *PCT Int Appl*, 171 pp. WO 2003080579 A1.

Franco R, Casado V, Mallol J, Ferre S, Fuxe K, Cortes A *et al*. (2005). Dimer-based model for heptaspanning membrane receptors. *Trends Biochem Sci* **30**: 360–366.

Gargett CE, Wiley JS (1997). The isoquinoline derivative KN-62 a potent antagonist of the P2Z-receptor of human lymphocytes. *Br J Pharmacol* **120**: 1483–1490.

Gever J, Cockayne D, Dillon M, Burnstock G, Ford APDW (2006). Pharmacology of P2X channels. *Pflügers Arch* **452**: 513–537.

Hibell AD, Thompson KM, Xing M, Humphrey PP, Michel AD (2001). Complexities of measuring antagonist potency at P2X(7) receptor orthologs. *J Pharmacol Exp Ther* **296**: 947–957.

Humphreys BD, Virginio C, Surprenant A, Rice J, Dubyak GR (1998). Isolquinolines as antagonists of the $P2X_7$ nucleotide receptor: high selectivity for the human versus the rat receptor homologues. *Mol Pharmacol* **54**: 22–32.

Jiang LH, Mackenzie AB, North RA (2000). Brilliant blue G selectively blocks ATP-gated rat P2X(7) receptors. *Mol Pharmacol* **58**: 82–88.

Michel AD, Chessell IP, Humphrey PP (1999). Ionic effects on human recombinant P2X7 receptor function. *Naunyn Schmied Arch Pharmacol* **359**: 102–109.

Michel AD, Kaur R, Chessell IP, Humphrey PP (2000). Antagonist effects on human P2X(7) receptor-mediated cellular accumulation of YO-PRO-1. *Br J Pharmacol* **130**: 513–520.

Michel AD, Miller KJ, Lundstrom K, Buell GN, Humphrey PP (1997). Radiolabeling of the rat p2x4 purinoceptor: evidence for allosteric interactions of purinoceptor antagonists and monovalent cations with p2x purinoceptors. *Mol Pharmacol* **51**: 524–532.

Michel AD, Thompson KM, Simon J, Boyfield I, Fonfria E, Humphrey Patrick PA (2006b). Species and response dependent differences in the effects of MAPK inhibitors on P2X7 receptor function. *Br J Pharmacol* **149**: 948–957.

Michel AD, Xing M, Thompson KM, Jones CA (2006a). Decavanadate, a P2X receptor antagonist, and its use to study ligand interactions with P2X7 receptors. *Eur J Pharmacol* **534**: 19–29.

Montminy MR, Sevarino KA, Wagner JA, Mandel G, Goodman RH (1986). Identification of a cyclic-AMP-responsive element within the rat somatostatin gene. *Proc Natl Acad Sci USA* **83**: 6682–6686.

Murgia M, Hanau S, Pizzo P, Rippa M, Di Virgilio F (1993). Oxidized ATP. An irreversible inhibitor of the macrophage purinergic P2Z receptor. *J Biol Chem* **268**: 8199–8203.

North RA (2002). Molecular physiology of P2X receptors. *Physiol Rev* **82**: 1013–1067.

Prinz H, Striessnig J (1993). Ligand-induced accelerated dissociation of (+)-*cis*-diltiazem from L-type Ca^{2+} channels is simply explained by competition for individual attachment points. *J Biol Chem* **268**: 18580–18585.

Rassendren F, Buell GN, Virginio C, Collo G, North RA, Surprenant A (1997). The permeabilizing ATP receptor, p2x7. Cloning and expression of a human cDNA. *J Biol Chem* **272**: 5482–5486.

Romagnoli R, Baraldi PG, Di Virgilio F (2005). Recent progress in the discovery of antagonists acting at P2X7 receptor. *Expert Opin Ther Patents* **15**: 271–287.

Surprenant A, Rassendren F, Kawashima E, North RA, Buell G (1996). The cytolytic p-2z receptor for extracellular ATP identified as a p-2x receptor (p2x(7)). *Science* **272**: 735–738.

Virginio C, Church D, North RA, Surprenant A (1997). Effects of divalent cations, protons and calmidazolium at the rat $P2X_7$ receptor. *Neuropharmacol* **36**: 1285–1294.

Wiley JS, Chen R, Wiley MJ, Jamieson GP (1992). The ATP4-receptor-operated ion channel of human lymphocytes: inhibition of ion fluxes by amiloride analogs and by extracellular sodium ions. *Arch Biochem Biophys* **292**: 411–418.